Journal of Cleaner Production 382 (2023) 134899

Contents lists available at ScienceDirect

Journal of Cleaner Production

journal homepage: www.elsevier.com/locate/jclepro

The impact of activation temperature and time on the characteristics and performance of agricultural waste-based activated carbons for removing dye and residual COD from wastewater

A. Vakili [a], A.A. Zinatizadeh [a,b,*], Z. Rahimi [a], S. Zinadini [a,b], P. Mohammadi [c], S. Azizi [d,e], A. Karami [a], M. Abdulgader [f,g]

[a] Department of Applied Chemistry, Faculty of Chemistry, Razi University, Kermanshah, Iran
[b] Environmental and Pollution Engineering Group, Environmental Research Center (ERC), Razi University, P.O. Box 67144-14971, Kermanshah, Iran
[c] Department of Environmental Health Engineering, School of Public Health, Kermanshah University of Medical Sciences, Kermanshah, Iran
[d] UNESCO-UNISA Africa Chair in Nanosciences and Nanotechnology, College of Graduate Studies, University of South Africa, Muckleneuk Ridge, PO Box 392, Pretoria, South Africa
[e] Nanosciences African Network (NANOAFNET), iThemba LABS-National Research Foundation, 1 Old Faure Road, Somerset West, 7129, PO Box 722, Somerset West, Western Cape, South Africa
[f] School of Engineering and Built Environment, Griffith University, Nathan Campus, QLD, 4111, Australia
[g] Department of Environmental Science, Faculty of Environment and Natural Resources, Wadi Al-Shatti University, Libya

ARTICLE INFO

Handling Editor: Mingzhou Jin

Keywords:
Colored wastewaters
Adsorption
Activated carbon
Physical activation
Agricultural waste

ABSTRACT

The release of colored compounds containing wastewaters into the environment and surface water resources is known as a serious threat to public health and aquatic ecosystems. Accordingly, in the present study, cost-effective and efficient activated carbons (ACs) were prepared employing agricultural wastes (walnut shell) over a two-stage physical activation under CO2 at various activation temperature (700–1000 °C) and time (30–120 min). The prepared ACs were characterized by various analyses of SEM, XRD, FTIR, BET, and also their adsorption performance was checked via the measure of methylene blue (MB) number in order to determine selected activated carbon. According to the reported results, the AC produced at the activation temperature and time of 900 °C and 60 min, respectively, indicated better physicochemical properties and more favorable performance compared to others. The selected AC had the highest BET surface area (S_{BET}) of 903.9 m^2/g and the greatest adsorption capacity of 307.4 mg/g as the MB number. Furthermore, the adsorption capacity as iodine number and pH of point of zero charge (pH_{PZC}) were reported to be 1150 mg/g and 4.6, respectively, for the selected AC. In the following, the performance of the selected AC was further evaluated as adsorption of synthetic (MB) and natural dyes from biologically treated wastewaters under different conditions. Maximum absorption capacity of the MB was obtained to be 307.45 mg/g at optimum conditions (the adsorbent dosage of 1 g/L, adsorbate concentration of 400 mg/L, contact time of 3 h, and agitation speed of 150 rpm). Moreover, the selected AC demonstrated appreciable performance at adsorbent dosage of 1 g/L and the contact time of 240 min using three biologically treated wastewaters. The highest adsorption capacity of 395.7 mg/g was obtained by the biologically treated baker's yeast wastewater as the adsorbate. The selected AC revealed the highest conformity with the Langmuir isotherm model ($R^2 = 0.9999$) and the Pseudo-second-order kinetic model ($R^2 = 0.9994$).

1. Introduction

Today, sanitary issue and preservation of hygienic drinking water have become the most pervasive challenge all over the world (Mpatani et al., 2021). On the other hand, the water bodies are being polluted rapidly by various pollutants especially dyeing compounds produced by textile, paper, plastics, and leather industries annually (Bhatnagar and Anastopoulos, 2017). These compounds are recalcitrant in nature, and cannot be degraded by biological treatment methods. The existence of such compounds in water sources prohibits light penetration, thereby,

* Corresponding author. Department of Applied Chemistry, Faculty of Chemistry, Razi University, Kermanshah, Iran.
E-mail address: zinatizadeh@razi.ac.ir (A.A. Zinatizadeh).

https://doi.org/10.1016/j.jclepro.2022.134899
Received 4 May 2022; Received in revised form 21 October 2022; Accepted 24 October 2022
Available online 9 November 2022

interferers the biological process severely (Zangeneh et al., 2019). Hence, prior the discharge of these dangerous pollutants into the receiving water bodies and surrounding environment, the efficient and sufficient treatment approaches must critically be adopted.

In line with this, a variety of technologies have been implemented to treat color containing wastewaters including chemical precipitation process, membrane filtration-based technology, ion exchange, electrolysis, coagulation, solvent extraction, and electrocoagulation (Juang and Shiau, 2000). Nonetheless, any of which possess shortcomings themselves, for instance, high costs related to energy consumption and the formation of by-products in the oxidation method, regeneration issue of adsorbent and subsequent disposal requirements in the ion-exchange process, the high production of sludge and formation of large particles in the coagulation/flocculation approach, the short half-life in the ozonation method and the concentrated sludge production in the membrane filtration-based technologies (Salleh et al., 2011). Advantages and disadvantages of the various technologies used for the dye removal is summarized in Table S1.

Adsorption processes as a reliable method are widely used to handle wastewater owing to having excellent advantages such as easy operation, cost-effectiveness, friendly environment, reduction in sludge production and disposal issues (Sharafi et al., 2016). In spite of the appreciable benefits, this technology suffers from some of drawbacks such as the high price of treatment due to difficulty in regeneration (Dawood and Sen, 2012). Hence, the inexpensive and locally available precursors can be employed for the production of the activated carbon to make the adsorption process economically viable. In this regard, various materials such as carbon nanotubes (Gupta et al., 2013), biopolymers (Wang et al., 2016), conducting polymers (Srivastava et al., 2015), activated carbon (Hadi et al., 2016) and clay (Anirudhan and Ramachandran, 2015) have been used as adsorbent to eliminate dyes from aqueous environments.

Generally, bio-sorption is defined as the removal of pollutants using inactive, non-living materials or with biological origin over a promising, cost-effective and fine eco-friendly process (Farooq et al., 2010). In the last decade, the CNTs were used intensively for removing organic and inorganic pollutants, and scavenging the dyeing compounds (Gupta, 2009). Apart from the CNTs, cellulose-based adsorbents were broadly applied to treat dyed wastewater (Wang et al., 2016).

In general, the biosorption offers the beneficial advantages over other technologies, for example, easy accessibility and almost without spending any cost to the precursors available mainly as wastes or by-products, and low sludge generation (Farooq et al., 2010). Furthermore, the biosorption-based processes are very rapid since non-living compounds act as an ion-exchange resin, and they don't need aseptic conditions. However, these processes have their own disadvantages such as the need to regeneration of the value-added pollutant like metal ions adsorbed on the relevant adsorbent in order to re-employ them. Biomass-derived adsorbents exhibit competitive adsorptive properties for elimination of various pollutants in the multi-component adsorption processes (Yazidi et al., 2020).

Among various adsorbents, activated carbons (ACs) are one of the most popular adsorbents used in a variety of applications owing to distinguished features like greatly developed porosity, large surface area, manipulatable properties of surface chemistry, and high surface reactivity (Vunain and Biswick, 2019). There are various carbonaceous materials used to prepare ACs that are including coal, wood, peat, and agricultural and agroforestry waste-based precursors especially lignocellulose by-products (Vunain and Biswick, 2019). Of which, coal, lignite, and wood are the most commonly used precursors for preparation of the activated carbon that are not cost effective and renewable (Shahkarami et al., 2015). In overall, the selection of the proper precursor in order to get a cost-effective AC depends definitely on its costs, accessibility, purity, the ease of manufacturing process, and target applications of the final product. Over current years, a large amounts of walnut shells based agricultural residues have been produced and disposed in an improper manner giving rise to wasting valuable resources and polluting environment. While, it can be seen as a valuable carbonaceous material with low ash contents to not only produce a value added and inexpensive product i.e. the activated carbon, but also preserve the environment from the pollution (Zhao et al., 2020).

Sun et al. physically prepared activated carbon using rubber-seed shell as precursor under steam to investigate adsorption capacity of methylene blue (MB) (Sun and Jiang, 2010). Based on the obtained results, the prepared activated carbon with specific surface area (S_{BET}) of 948 m^2, iodine number of 1326 mg/g, and total pore volume of 0.988 cm^3/g displayed adsorption capacity of 265 mg/g. Ma et al. physically produced mesoporous activated carbon from precursor of Sargassum Fusiforme under oxidizing gas of CO_2 to study adsorption behavior on Congo red (Ma et al., 2020). Although the prepared activated carbon possessed high surface area (1329 m^2/g) and total pore volume (1.18 cm^3/g), the adsorption capacity was not as high as 265 mg/g. The removal rate at equilibrium conditions and the greatest adsorption capacity were reported to be 94.72% and 234 mg/g, respectively, at initial concentration of adsorbate (Congo red) of 200 mg/L, adsorbent dosage of 0.8 g/L, temperature of 30 °C, and pH of 7. Kumar et al. used Fox nutshell as precursor to chemically prepare activated carbon with high surface area (2869 m^2/g) and total pore volume (1.96 cm^3/g) by zinc chloride as activator at activation temperature and impregnation ratio of 600 °C and 2, respectively (Kumar and Jena, 2016). The adsorption capacity of the activated carbon was reported to be 968.74 mg/g. From the results, an increase in the equilibrium adsorption (q_e) of MB was observed ranged from 249.88 to 968.74 mg/g, once initial concentration of adsorbate was incremented from 100 mg/L to 500 mg/L Özhan et al. chemically prepared pine cone-based activated carbon prepared using $ZnCl_2$ activator under microwave radiation (Özhan et al., 2014). The BET surface area, total pore volume and iodine number obtained for this activated carbon were 939 m^2/g, 0.172 cm^3/g and 1360 mg/g, respectively. Adsorption capacity was obtained to be 60.97 mg/g using MB as model dye. In all these studies, the agricultural wastes have been used as precursor in the production of the activated carbon under physical and chemical activation methods. Also, in most of these researches, methylene blue dye has been used as an adsorbate. Activated carbons produced by the physical activation method have shown almost equal adsorption capacity. However, in the case of chemically produced activated carbons, although the same activator i.e. zinc chloride was used in both studies, significant differences in surface properties and adsorption capacity have been shown. This may be due to type of the precursors used in the production of these activated carbons. In addition, the physical activation method is more favorable compared to the counterpart method environmentally and economically since it does not need to use chemicals, therefore, not produce secondary pollution.

Inspired from the earlier studies conducted in this area, we were encouraged to physically prepare the sufficient activated carbons using walnut shell as an agricultural waste based precursor which is locally abundant and easily accessible to remediate dyes from the synthetic and real samples. In this regards, the relevant activated carbons were prepared under different activation temperatures (700, 800, 900, 1000 °C) and times (30, 60, 90 and 120 min) under CO_2 gas flow to enhance adsorption capacity. The prepared activated carbons were characterized using analysis of BET, FT-IR, XRD and SEM. Firstly, the performance of the resultant activated carbons was investigated as adsorption capacity and dye removal using methylene blue (MB) as model dye. The methylene blue (MB) number means the adsorption capacity of the activated carbon using the methylene blue dye. From the literature, methylene blue (MB) number (Jiang et al., 2019) and iodine number (Kaya et al., 2018) are measured in the adsorption processes to investigate the adsorption performance of the activated carbon in liquid phase. Accordingly, in this study, the adsorption performance of the selected activated carbon was evaluated using these two parameters. Given that the presence of natural dye and residual COD in the biologically treated wastewaters is known as a big dilemma against the water reuse,

Table 1
Compositions of the biologically treated wastewaters.

Type of real sample	COD (mg/L)	pH
Baker's yeast effluent	875.3	7.2–8
Licorice processing effluent	205.85	6.5–7
Waste stabilization pond's effluent	160.73	7–7.5

therefore, the novelty of the present study is related to the investigation of the performance of the selected AC produced from the walnut shell precursor as removal of concerned pollutants from the pre-treated field samples. The real samples used as adsorbate were including the biologically treated wastewaters i.e. baker's yeast wastewater, municipal wastewater treated by waste stabilization pond (WSP) and licorice processing wastewater. Finally, kinetic and isotherm studies were accomplished for the selected activated carbon.

2. Materials and methods

2.1. Materials

In present work, walnut shell (WS) as a precursor was collected from local farms (Songhor, Kermanshah, Iran). Nitrogen (N_2, purity of 99.9999%) and carbon dioxide (CO_2, purity of 99.9999%) gases were used as inert gas at carbonization stage and oxidizing agent at activation stage, respectively. Methylene blue dye ($C_{16}H_{18}N_3ClS$, molecular weight of 319.85) as model dye was purchased from Merck Com., Germany. The characteristics of biologically treated wastewater namely baker's yeast, waste pond stabilization (WPS) and licorice effluents are given in Table 1.

2.2. Preparation of activated carbon

In principle, the production of activated carbon using physical method can be conducted over two stages, carbonization and activation stages (Hindarso et al., 2001). According to Yagmur et al. the aim of the carbonization stage is to increment the fixed carbon contents and make the produced char porous somehow under the inert atmosphere of N_2 via eliminating non-carbon materials as gas and tars (Yagmur et al., 2008). The char produced in this stage has low surface area, and is not active. While, the activation stage is carried out under oxidizing environment of CO_2, air or steam to create pores and vessels in the resultant activated carbon as a result of the entrance of the oxidizing gas into the activated carbon texture leading to the development of the surface area and porosity.

2.2.1. Carbonization stage

Before the char production, the walnut shells (WS) were washed with hot distilled water to eliminate impurities, and dried at 110 °C for a day. Then, they were powdered using a roller mill and sieved to mesh 400. Next, the powdered walnuts shells were characterized as moisture, volatile matter, fixed carbon and ash content according to ASTM techniques (Heidari et al., 2014).

The pyrolysis process was performed in an electric furnace (BATEC, PC21-A) under the inter gas stream of N_2 with a flow rate of 500 mL/min and operating pressure of 1.5 bar. A certain amount of raw precursor was heated from room temperature to the final carbonization temperature of 600 °C with heating rate of 10 °C/min and the activation time of 60 min. After finishing the activation time, the produced char was cooled under N_2 gas to ambient temperature (Nowicki et al., 2010).

2.2.2. Activation stage

To prepare the activated carbon, a pre-weighted amount of the produced char was placed in the electric furnace. Before the activation process, the furnace was firstly purged with N_2 gas stream for almost 30 min to guarantee an inert atmosphere. Consequently, the furnace was heated at a constant heating rate of 10 °C/min to different activation temperature of 700–1000 °C for the varied activation time (30–120 min) under the CO_2 gas stream with the flow rate of 500 mL/min, operating pressure of 1.5 bar and high purity (99.99999%). The CO_2 gas for the activation process was chosen based on the literature (Danish and Ahmad, 2018; Yahya et al., 2015). After activation time, the prepared activated carbons were allowed to be cooled under the N_2 atmosphere to the ambient temperature. To remove the impurity and produced ash, the activated carbons were washed with the distilled water and air-dried in an oven at 110 °C for 24 h. Then, yield (wt. %) of the prepared activated carbons was measured by dividing the mass of prepared activated carbon by the mass of the dried precursor (Álvarez-Gutiérrez et al., 2015). In this section, the range of studied variables was chosen based on the typical range reported in earlier works (Karaman et al., 2014). The stages of the activated carbon preparation are displayed schematically in Fig. S1.

2.3. Characterization

The surface morphologies of the activated carbon samples were examined through the SEM images taken by scanning electron microscopy (SEM, KYKY-EM3200, China). The functional groups of the prepared activated carbons were characterized by the measure of FTIR spectra (FTIR - AVATAR 370, Thermo Nicolet) in the range of 4000–400 cm^{-1}. The textural and structural attributes of the prepared samples were investigated through N_2 gas adsorption at 77 K in a gas adsorption analyzer (Micromeritics ASAP 2010; Japan) after outgassing the sample for 2 h at 523 K. The specific surface area of the samples was analyzed by the N_2 adsorption isotherms applying the Brunauer–Emmett– Teller (BET) equation (Ghouma et al., 2015). Additionally, the amorphous and crystalline nature of the acquired samples was characterized via X-ray diffraction (XRD, (Philips Xpert MPD diffractometer) by Cu at diffraction angles (2θ) of 10–100 (Beyan et al., 2021). The point of zero charge (pHpzc) of the selected activated carbon was calculated by employing a batch equilibrium approach. Moreover, iodine number was measured for the selected activated carbon as adsorptive capacity of iodine using the sodium thiosulfate volumetric method (Demiral et al., 2011).

2.4. The performance assessment of the prepared activated carbons

The performance of the prepared activated carbons was investigated according to the procedure followed by Kumar et al. (Kumar and Jena, 2016). This section is including three steps. At first step, the functionality of the various activated carbons (ACs) prepared under varied experimental conditions were assessed using synthetic methylene blue (MB) dye in terms of dye removal efficiency and adsorption capacity to reach the selected activated carbon. For this purpose, different concentrations of the MB dye ranging from 100 to 700 mg/L were prepared and the performance of the whole activated carbons was checked as the targeted parameters (the dye removal efficiency and the adsorption capacity) at regular contact time intervals of 5–240 min. Following this part, the performance of the selected AC was further investigated under variables commonly studied at adsorption experiments i.e. agitation speed (50–250 rpm), solution pH (2–12), adsorbent dosage (0.2–1.6 g/L), initial adsorbate concentrations (100–700 mg/L) and contact times (5–240 min) using the MB dye to attain the optimum experimental conditions. At the entire experiments, the dye removal efficiency and the adsorption capacity were measured. At third step, the performance of the selected AC was examined as the dye removal efficiency, chemical oxygen demand (COD) removal efficiency and the adsorption capacity in terms of COD using the biologically treated wastewaters, namely, effluents from waste stabilization pound (WSP) containing algal dye, licorice processing and baker's yeast wastewaters (see Table 1). In this step, the impact of the contact time (15–240 min) and the adsorbent dosage (0.33, 0.5 and 1 g/L for effluents from waste stabilization pond (WSP) and the biologically treated licorice processing wastewater, and

Table 2
The results of component analysis and approximate analysis obtained for walnut shell precursor as wt. %.

Approximate analysis	
Moisture	2.13
Ash	1.12
Volatile matter	77.94
Fixed carbon	18.81
Component analysis	
Extractives	5.5
Cellulose	33.13
Lignin	31.86
Hemicellulose	29.51

1, 2 and 3 g/L for the effluent from the biologically treated baker's yeast processing wastewater) were examined on the performance of the selected activated carbon. The dye removal efficiency and the adsorption capacity were computed the equations below (Calvete et al., 2010).

$$R = \frac{(C_0 - C_e)}{C_0} \times 100 \quad (1)$$

$$q_e = \frac{(C_0 - C_e) \times V}{ms} \quad (2)$$

here, R, C_0 and C_e are the dye removal efficiency (%), the initial and equilibrium adsorbate concentrations (mg/L), respectively. q_e, V and m_s refer to the equilibrium adsorption capacity (mg/g) as the MB dye and COD, solution volume (L) and adsorbent dosage (g), respectively. The absorbance of the synthetic and natural dye samples was determined at a certain wavelength of 664 nm and in the range of visible wavelengths (400–800 nm), respectively.

2.5. Adsorption kinetic studies

There are several models employed to describe the controlling mechanism of adsorption process using the obtained laboratory data (Mahmoodi et al., 2011). In this regard, intraparticle diffusion model was used to check intraparticle diffusion resistance influencing the adsorption process. The intraparticle diffusion model was defined as follow:

$$q_t = K_p t^{0.5} + C \quad (3)$$

where, q_t, K_p, $t^{0.5}$ and C are defined as the adsorption capacity (mg/g) at time t (min), rate constant of the intraparticle diffusion (mg/g $min^{1/2}$), half-time ($min^{0.5}$) and the intercept, respectively. In this model, C parameter is indicator of the thickness of the boundary layer. From this model, if the graph becomes linear, the intraparticle diffusion model will play a significant role in the adsorption process. In addition, this model will be the rate controlling step if these straight lines pass through the origin, if not, this is revealing some degrees of the boundary layer control. This result further indicates that the rate controlling step is not only governed by the intraparticle diffusion model, but also other kinetic models may be incorporated (Mahmoodi et al., 2011). The other kinetic models i.e. pseudo-first order and the pseudo-second order equations are described employing equations (4) and (5), respectively.

$$ln(q_e - q_t) = ln\ q_e - k_1 t \quad (4)$$

where, q_e and k_1 stand for the adsorption capacity at equilibrium conditions (mg/g) and the equilibrium rate constant (1/min), respectively.

$$\frac{t}{q_t} = \frac{1}{K_2 q_e^2} + \left(\frac{1}{q_e}\right) t \quad (5)$$

where, q_e and q_t are the adsorption capacity (mg/g) at equilibrium conditions and time t, respectively. t and K_2 refer to time (min) and kinetic rate constant (g/min/mg), respectively.

2.6. Adsorption isotherm

The modeling of adsorption isotherms was conducted by three popular models i.e. the Langmuir, Freundlich, and Temkin. The Langmuir isotherm is based on assumption of uniform energy of the adsorption process without interacting adsorbate–adsorbate (Langmuir, 1918). The adsorption energy remains constant in the whole adsorption sites and the adsorption process takes place as monolayer (Tonucci et al., 2015). The expression of Langmuir isotherm is described as the following equation.

$$q_e = \frac{q_m K_L C_e}{1 + K_L C_e} \quad (6)$$

here, K_L, q_e and q_m are defined as Langmuir constant (L/mg) showing the energy adsorption, adsorption capacities at equilibrium conditions and maximum state (mg/g), respectively. C_e expresses concentration of the MB (mg/L) at the equilibrium state. The Langmuir equation can be rewritten as liner form as follows.

$$\frac{C_e}{q_e} = \frac{1}{K_L q_m} + \frac{C_e}{q_m} \quad (7)$$

The desirability of the adsorption process is investigated as the values of separation factor (R_L, dimensionless) determined using equation (5) (Acero et al., 2012). So that if the values of R_L lie between 0 and 1 ($0 < R_L < 1$), the adsorption process is favorable. The value of R_L above 1 is indicating unfavorable adsorption process. If values of R_L equal to 1 or 0, the adsorption process will be linear or irreversible, respectively.

$$R_L = \frac{1}{1 + K_L C_0} \quad (8)$$

The Freundlich isotherm assumes the adsorption process happens heterogeneously, and does not regard the saturation of the adsorption surface (Tonucci et al., 2015). The Freundlich model is presented as follows.

$$q_e = K_F C_e^{\frac{1}{n}} \quad (9)$$

here, K_F and n are representative of the adsorption capacity and adsorption intensity, respectively. The Freundlich model can be linear by taking Ln of both sides of equation (9) given in the following equation.

$$ln\ q_e = ln\ k_F + \frac{1}{n} ln\ C_e \quad (10)$$

The Temkin model relies on assumption of the linear mitigation in adsorption heat of the whole adsorbed molecules with the coverage as a result of interacting adsorbate–adsorbate. The Temkin isotherm is demonstrated by equation (11).

$$q_e = \frac{RT}{b_T} ln(AC_e) \quad (11)$$

where, T and R, A and b_T represent temperature (K), gas constant (J/mol.K), Temkin constant (L/mg) and the adsorption heat (J/mol), respectively. The linear form of Temkin equation is demonstrated as the following equation.

$$q_e = B\ ln(A) + B\ ln\ C_e \quad (12)$$

$$B = \frac{RT}{b_T}$$

3. Results and discussion

3.1. Approximate and component analysis of walnuts shells precursor

The results of approximate analysis measured for walnut shell

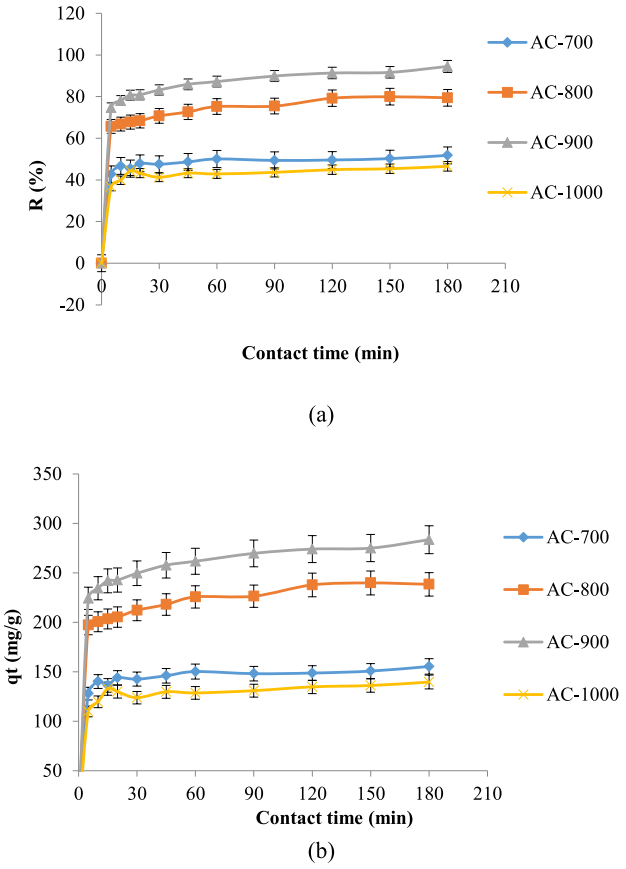

Fig. 1. (a) The dye removal efficiency and (b) adsorption capacity measured for the selected activated carbon at activation time of 60 min and various activation temperatures using the MB (solution volume of 100 mL; initial adsorbate concentration of 300 mg/L; adsorbent dosage of 0.1 g; solution pH of 6–7; agitation speed of 150 rpm at ambient temperature).

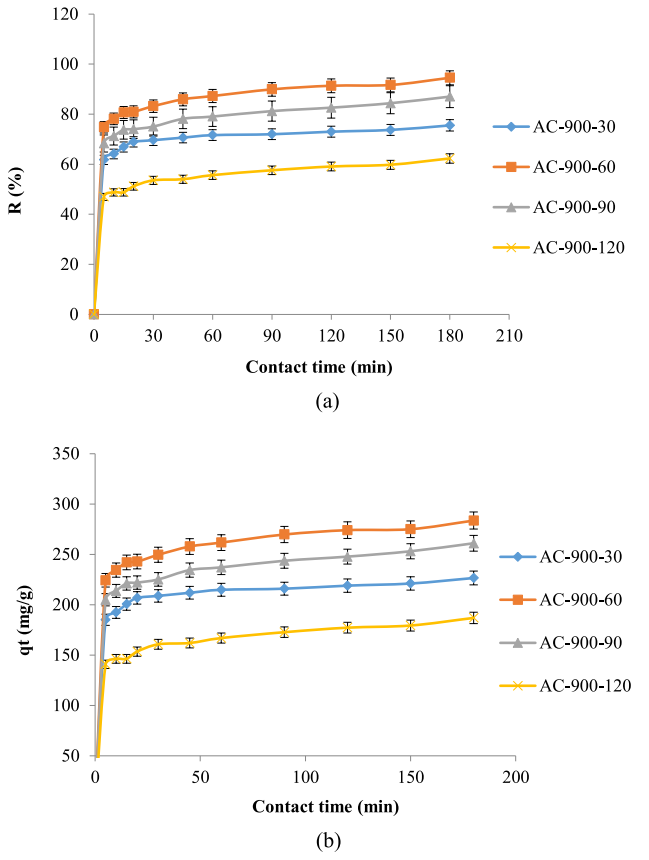

Fig. 2. (a) The dye removal efficiency and (b) adsorption capacity measured for the selected activated carbon at optimum activation temperature of 900 °C and various activation times using the MB (solution volume of 100 mL; initial adsorbate concentration of 300 mg/L; adsorbent dosage of 0.1 g; solution pH of 6–7; agitation speed of 150 rpm at ambient temperature).

precursor are present in Table 2. From the Table, the high amount of volatile matter (77.94 wt %) and fixed carbon (18.81 wt %) while low amount of moisture (2.13 wt %) and ash content (1.12 wt %) are strong evidence showing walnut shell biomass is a good option for preparation of AC (Nowrouzi et al., 2017). Moreover, component analysis was conducted for the concerned precursor. The acquired data are given in Table 2. It is documented that the raw bio-materials that have noticeable contents of hemicelluloses and cellulose are favorable to fabricate sufficient ACs (Heidari et al., 2014). The characterization of the prepared activated carbons is described in supporting information (SI) in Figs. S2–S7 and Tables S2–S4.

3.2. Evaluation of performance of various activated carbons using methylene blue (MB)

The productivity of different activated carbons prepared under various conditions was investigated as the dye removal efficacy and adsorption capacity using the MB as the model synthetic dye in order to identify the selected activated carbon during batch experiments. The data obtained for the dye removal efficiency (R as %) and the adsorption capacity as a function of time (q_t as mg/g) for the activated carbons prepared at the activation time of 60 min and different activation temperature are presented in Fig. 1. The outcomes indicate that with the increase in the activation temperature up to 900 °C, the capability of the dye removal and adsorption capacity both promote, whereas, further increase of temperature to 1000 °C leads to a reverse impact on the studied responses. The highest dye removal efficiency and adsorption capacity were 94.51% and 283.53 mg/g, respectively. Therefore, the activated carbon fabricated at the activation temperature of 900 °C was regarded as the selected activated carbon. At the next stage, the impact of activation time would be surveyed on the various activated carbons to find the optimum activation time.

The dye removal efficiency and adsorption capacity acquired for the activated carbons fabricated at optimum activation temperature (900 °C) and the different activation time are represented in Fig. 2. As evident from the Figure, elevating the activation time up to 60 min brings about the improvement in the investigated responses. In contrast, at the activation time above 60 min, a downward trend was observed in both parameters. Consequently, the activation time of 60 min is recognized as optimum time. Totally, according to the findings, the activated carbon prepared at the activation temperature and time of 900 °C and of 60 min is considered as the selected activated carbon. The largest dye removal efficiency and adsorption capacity are reported to be 94.51% and 283.53 mg/g, respectively.

From the literature, the most significant feature of the activated carbon is attributed to the adsorption capacity, proportional with the BET surface area (Shoaib and Al-Swaidan, 2015). The activation time and temperature are known as two effective factors in the increase of the BET surface area and the total pore volume to some extent. These two parameters confirm the role of burn-off on the increase of the BET surface area and the total pore volume. The increase in the activation time and temperature, which in turn, the increase in the burn-off leads to the creation of the meso- and micro-pores and therefore the enhancement in the BET surface area and the total pore volume via burning carbon and removing particles. However, the further increase in the activation time and temperature results in the destruction of porosity by external

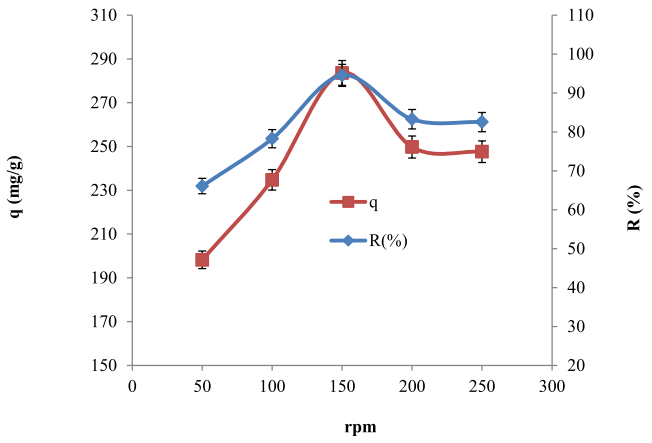

Fig. 3. The impact of the agitation speed on the adsorption capacity and dye removal efficiency using MB dye for the selected activated carbon (initial adsorbate concentration of 300 mg/L; solution volume of 100 mL; adsorbent dosage of 0.1 g; contact time of 180 min, solution pH of 6–7 at ambient temperature).

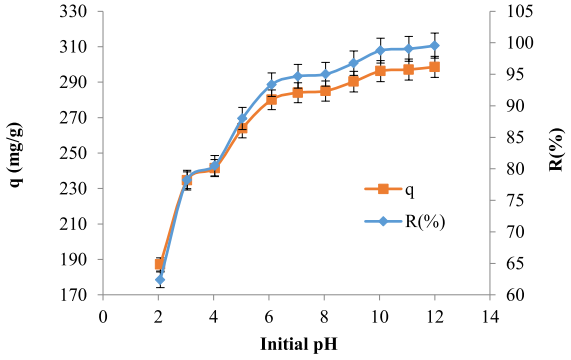

Fig. 4. The impact of the solution pH on the adsorption capacity and dye removal efficiency using MB dye for the selected activated carbon (initial adsorbate concentration of 300 mg/L; solution volume of 100 mL; adsorbent dosage of 0.1 g; contact time of 180 min, agitaion speed of 150 rpm at ambient temperature).

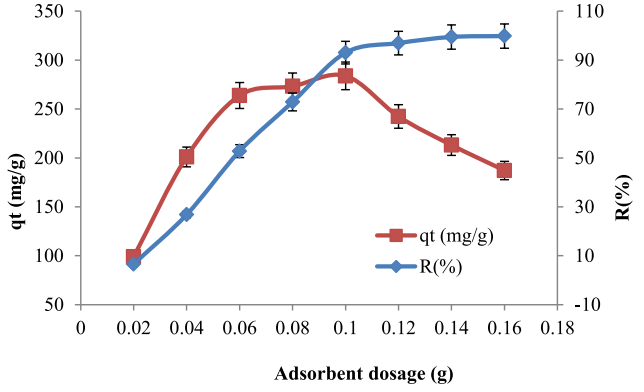

Fig. 5. The impact of the adsorbent dosage on the adsorption capacity and dye removal efficiency using MB dye for the selected activated carbon (initial adsorbate concentration of 300 mg/L; solution volume of 100 mL; contact time of 180 min, pH solution of 6–7; agitaion speed of 150 rpm at ambient temperature).

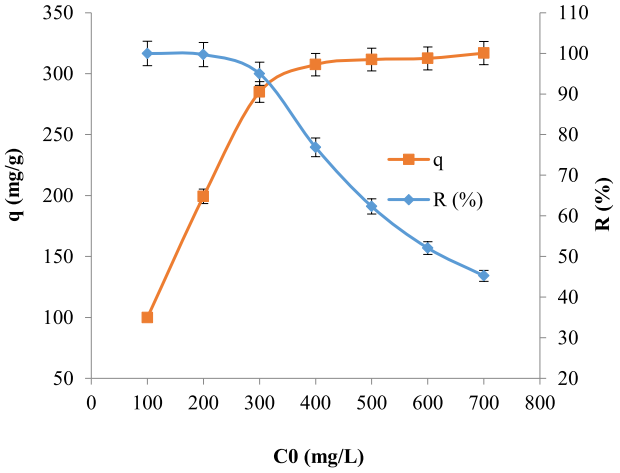

Fig. 6. The impact of the initial concentration of adsorbate on the adsorption capacity and dye removal efficiency using MB dye for the selected activated carbon (adsorbent dosage of o.1 g; solution volume of 100 mL; contact time of 180 min, pH solution of 6–7; agitaion speed of 150 rpm at ambient temperature).

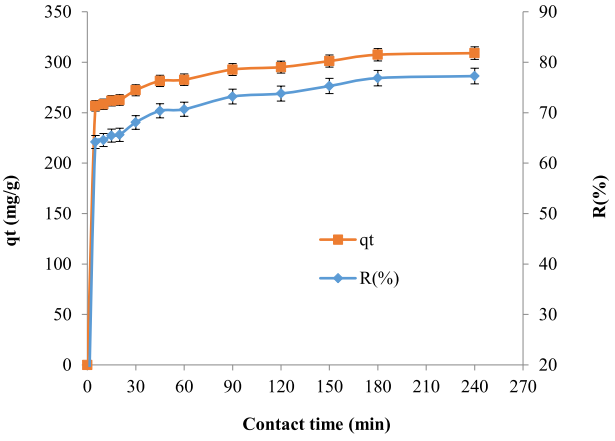

Fig. 7. The impact of the contact time on the adsorption capacity and dye removal efficiency using MB dye for the selected activated carbon (adsorbent dosage of o.1 g; adsorbate concentration of 400 mg/L; solution volume of 100 mL; pH solution of 6–7; agitaion speed of 150 rpm at ambient temperature).

Table 3
The findings obtained from kinetic parameters of pseudo-first-order, pseudo-second-order and intraparticle diffusion models.

Kinetic model	Parameter	Value
pseudo-first-order	R^2	0.9854
	K_1, (1/min)	0.014
	Calculated qe, (mg/g)	55.191
pseudo-second-order	R^2	0.9994
	K_2, (g/(mg min)	0.00084
	Calculated qe, (mg/g)	312.5
Intraparticle diffusion	R^2	0.9723
	Ki	4.3783
	C	247.03

Table 4
The results of various isotherm parameters.

Type of isotherm model	Parameter	Value
Langmuir	R^2	0.9999
	k_L، (L/mg)	0.7273
	q_m ، (mg/g)	312.5
Freundlich	R^2	0.8877
	k_F ، (mg/g(L/mg))$^{1/n}$	174.214
	n	8.5616
Tempkin	R^2	0.9492
	B	23.22
	A، (L/g)	4169.83

Table 5
The comparison of the specific surface area and adsorption capacity obtained for the agricultural waste-based activated carbons for adsorption of the methylene blue from aqueous solutions.

Type of precursor	Synthesis method	S_{BET}, m^2/g	Adsorption capacity, mg/g	References
Cotton cake	Chemical (H_3PO_4)	584	250	Ibrahim (2014)
Bamboo	Chemical (H_3PO_4)	1335	183.3	Liu et al. (2010)
Walnut shell	Chemical ($ZnCl_2$)	1800	315	Yang and Qiu (2010)
Rice husk	Chemical (K_2CO_3)	1713	210	Liu et al. (2012)
Coffee husks	Chemical ($FeCl_3$)	956	75	Oliveira et al. (2009)
Sunflower oil cake	Chemical (H_2SO_4)	240	16.4	Karagöz et al. (2008)
Date pits	Chemical ($FeCl_3$)	780	259.25	Theydan and Ahmed (2012)
Rice straw	Chemical (H_3PO_4)	522	109.1	Fierro et al. (2010)
Waste apricot	Chemical ($ZnCl_2$)	1060	316.9	Başar (2006)
Orange peels	Chemical (K_2CO_3)	543.89	243.66	Foo and Hameed (2012)
Coconut shell	Chemical (NaOH)	876.13	200.01	Islam et al. (2017)
Weeds	Chemical (HNO_3)	5.138	92.59	Güzel et al. (2017)
Municipal solid wastes	Chemical (KOH)	662.4	21.83	Sumalinog et al. (2018)
Wood furniture waste	Physical (CO_2)	855	200	Sainz-Diaz and Griffiths (2000)
Urban sewage sludge	Physical (CO_2)	168	120	
Tire waste	Physical (CO_2)	289	130	
Coconut shell	Physical (steam)	–	277.9	Kannan and Sundaram (2001)
Groundnut shell	Physical (steam)	–	164.9	
Bamboo dust	Physical (steam)	–	143.2	
Walnut shell	Physical (CO_2)	903.911	307.45	The present study

ablating the carbon particles and vanishing the meso- and micro-pores. In other words, during over-burning reactions, the macro-pores are formed. Thereby, the BET surface area, micro-pores and the total pore volume are decreased. These outcomes show a good consistent with those achieved from the characterization analysis as described in the previous sections. Totally, the adsorption capacity of the activated carbon is known as the most important feature related to the surface area. As mentioned previously, the BET surface areas of the activated carbons increased with the increase in activation time and temperature to 60 min and 900 °C, respectively. In addition, the pore volume of the activated carbon is also a significant factor in the removal of pollutants. In this study, total pore volumes and BET surface area increased up to the optimum activation time (60 min) and temperature (900 °C) due to the reasons explained in the earlier sections. Generally, the increase in the mesoporosity volume enhances the absorption capacity as methylene blue (Kaya et al., 2018). Based on the data obtained from BET analysis, the percentage of mesopore volume for the selected activated carbon (62.4%) is less than the activated carbon prepared at the activation temperature and time of 1000 °C and 60 min, respectively, (74.1%). Nonetheless, the highest absorption capacity of methylene blue was reported to be for the optimum activated carbon (283.53 mg/g), ascribed to the increase of the mesoporosity volume of the selected active carbon (0.38245 cm^3/g) compared to the activated carbon prepared at prepared at the activation temperature and time of 1000 °C and 60 min (0.18547 cm^3/g). These results are consistent with the results obtained from the other work (Kaya et al., 2018).

The selected activated carbon, on the other hand, possesses a higher specific surface area (903.9 m^2/g) compared to others. Therefore, it can be concluded that the increment in the specific surface area is a dominant factor in the enhancement of the dye removal efficacy and adsorption capacity using the MB. According to Jia et al. when the Hg^0 as adsorbate contacted with the adsorbent, the adsorption process happened via internal mass transfer mainly including surface adsorption and pore diffusion (Jia et al., 2021). The surface adsorption and the pore diffusion mechanisms could be enhanced by developing the surface chemical characteristics and the pore structure, respectively. Thereby, the occupation rate of the adsorption active sites was increased. The adsorption reactions started firstly with the surface adsorption mechanism and the reaction progressed until the adsorbate covered fully the adsorbent surface. In this situation, the adsorbate couldn't contact with the activated carbon surface directly, however, the adsorption process continued through the pore diffusion mechanism. In the case of the MB, according to the literature, there are various mechanisms to adsorb this adsorbate that are 1) pore-filing mechanism through the meso-pores, 2) formation of the hydrogen bonding between the nitrogen atom from the MB and oxygen containing functional groups on the surface of the activated carbon, 3) Yoshida hydrogen bonding between the aromatic rings of MB and the O–H functional groups of the activated carbon, 4) electrostatic attraction between the negatively charged adsorbent surface and the MB cations, 5) π–π interaction, and 6) the van der Waals forces (Binh and Kajitvichyanukul, 2019).

3.3. The impact of different variables on the functionality of selected activated carbon

3.3.1. Agitation speed

The agitation speed influences the external boundary film and the distribution of the solute in the bulk solution during batch experiments significantly (Kumar and Jena, 2016). Fig. 3 displays the impact of the agitation speed (50,100,150, 200, 250 rpm) on the dye removal and adsorption capacity (q (mg/g)) using methylene blue (MB) as model synthetic dye for the selected activated carbon. The outcomes indicate that the increase in the agitation speed up to 150 rpm gave rise to the increase in the dye removal efficiency and adsorption capacity. The largest adsorption capacity and dye removal efficiency were 283.59 mg/g and 94.53%, respectively. These findings correlate that the optimum agitation speed (150 rpm) reduced the diffusion resistance of the MB ions towards the activated carbon surface due to formation of a uniform suspension of the activated carbon and relevant adsorbate (MB molecules) (Kumar and Jena, 2016). At the agitation speeds over 150 rpm, the amount of the MB adsorption lessens ascribed to the vortex phenomenon and the lack of adequate accessibility of the MB molecules to the activated carbon adsorbent (Abbas and Trari, 2020). Therefore, this moderate agitation speed (150 rpm) provides a good homogeneity for the suspension of the activated carbon and dye molecules and prevents the vulnerable phenomenon of vortex.

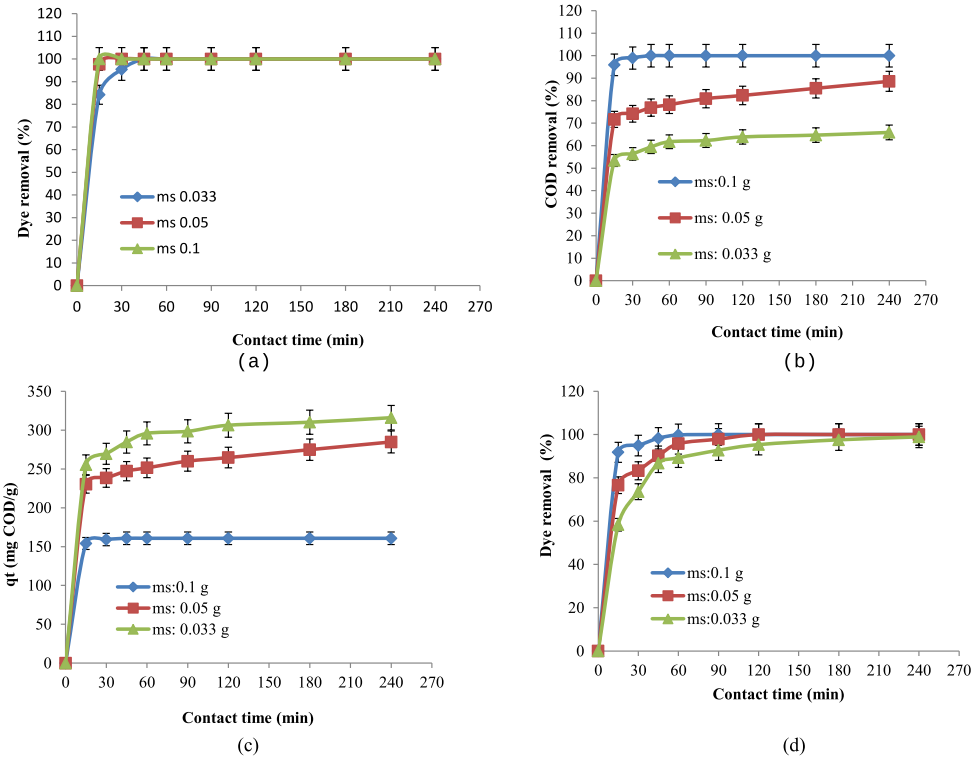

Fig. 8. The dye removal efficiency, the COD removal efficiency, and the COD adsorption capacity obtained from effluents of (a, b, c) algal dye containing waste stabilization pound; (d, e, f) biologically treated licorice processing wastewater; (g, h, i) biologically treated baker's yeast processing wastewater (agitation speed of 150 rpm, contact time of 15–240 min at ambient temperature).

3.3.2. Solution pH

In this study, the impact of solution pH ranging from 2 to 12 on the adsorption capacity and dye removal efficiency of the MB molecules using the selected activated carbon under optimum agitation speed of 150 rpm obtained from previous sections was examined and the findings are indicated in Fig. 4. From the Figure, two studied parameters, i.e. the adsorption capacity and dye removal efficiency, indicated a direct relationship with the increase in pH. The maximum amounts of the adsorption capacity and dye removal efficiency of 298.605 mg/g and 99.54%, respectively, were related to pH of 12. Underlying causes for such results can be described by pH of the point of zero charge (pH_{PZC}) and the physicochemical properties of the methylene blue as adsorbate. Methylene blue is a cationic dye and its adsorption on the adsorbent (activated carbon) is effected by the variation in the solution pH (Gokce and Aktas, 2014). At pHs over pH_{PZC}, the activated carbon surface possesses negative charge, and while at pHs less than pH_{PZC}, the activated carbon surface becomes positive (Abbas and Trari, 2020). Based on these mechanisms, at low pHs, a repulsive force is predominant between positively charged components i.e. the activated carbon and dye molecules. Reduction in the adsorption capacity and dye removal at low pH is owing to the increase in proton ions (H^+) in activated carbon-methylene blue suspension and their competition with methylene blue cations to be adsorbed on the activated carbon surface. On contrary, once the solution pH increases, the number of positively charged species diminish, and negatively charged adsorbent surface tends to uptake more the methylene blue cations via electrostatic attraction (Abbas et al., 2014). As far as, by increasing the solution pH, the remarkable change was not observed in the uptake of the MB, the pH of the dye solution itself that was around 6–7 was considered as the optimum value.

3.3.3. Adsorbent dosage

Determining the optimum dosage of adsorbent is a significant factor from economic view (Salleh et al., 2011). In this study, the effect of the adsorbent dosage ranging from 0.2 to 1.6 g/L with adsorbate concentration of 300 mg/L at optimum values of pH (6–7) and agitation speed of 150 rpm was explored on the studied parameters i.e. the dye removal efficiency and adsorption capacity of the MB molecules. The attained data are portrated in Fig. 5. From the experimental data, that is evident that by increasing the amount of activated carbon as adsorbent from 0.2 to 1.0 g/L, the dye removal efficiency and the adsorption capacity elevated from 6.5% to more than 93% and from 98.9 to 283.9 mg/g, respectively. In contrast, with further increment in the content of adsorbent from 1.0 g to 1.6 g/L, the dye removal efficiency did not change drastically. Totally, the dye removal efficiency shows a direct relationship with increasing absorbent dosage ascribed to the increase in the active sites of the activated carbon available for adsorbate molecules (Olusegun and Mohallem, 2020). But there is a reverse trend for the adsorption capacity with further increasing the adsorbent dosage. Once the amount of activated carbon increases from 1.0 g to 1.6 g/L, the adsorption capacity mitigated to 183.17 mg/g. This observation is justified by the greater active sites number of adsorbent in aqueous medium compared to the number of dye molecules, consequently, many active sites remain unused (Foroutan et al., 2021). In overall, at high adsorbent dosages, two factors i.e. overlapping of the active sites or insufficient concentration of adsorbate in the aqueous solution to interact with active and accessible sites on the adsorbent surface lead to the reduction in the adsorption capacity (Foroutan et al., 2019). From the outcomes, the amount of 1.0 g/L was considered as the optimum value of the adsorbent dosage.

3.3.4. Initial concentration of the adsorbate

One of the upmost significant factors influencing the adsorption

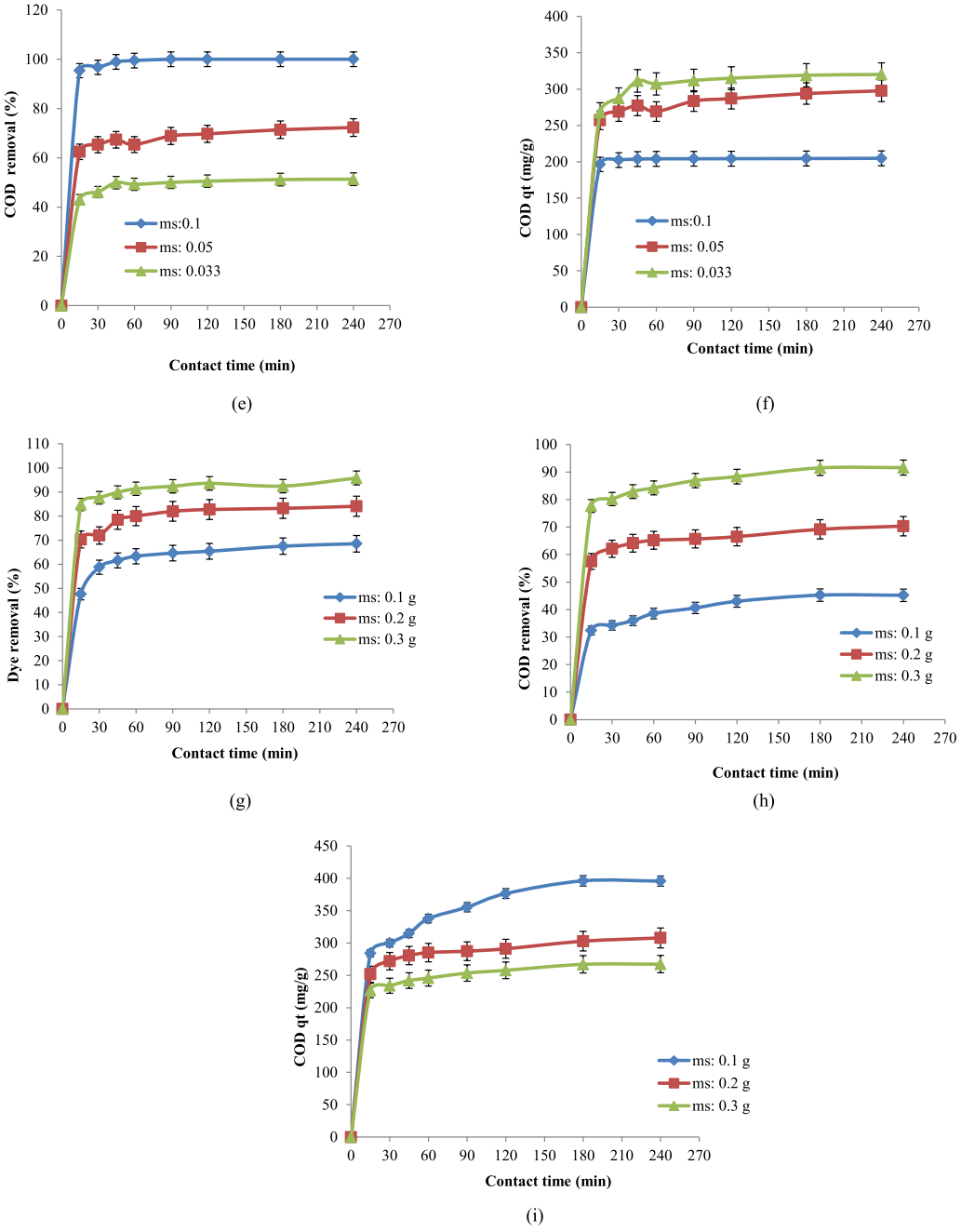

Fig. 8. (*continued*).

capacity and the dye removal efficiency is the initial concentration (C_0) of the adsorbate (Bulut and Aydın, 2006). Accordingly, impact of initial concentration of adsorbate, here MB, (100, 200, 300, 400, 500, 600 and 700 mg/L) on the adsorption capacity and the dye removal efficiency using the selected activated carbon prepared at activation temperature and time of 900 °C and 60 min, respectively, in pre-determined optimal experimental conditions (absorbent dosage of 1.0 g/L, agitation speed of 150 rpm and solution pH of 6–7) is showcased in Fig. 6. From the literature, methylene blue (MB) number (Benadjemia et al., 2011) and iodine number (Kaya et al., 2018) as adsorption capacity together form an effective approach to investigate the adsorption performance of activated carbon in liquid phase. From the obtained data, the increment in the initial concentration of dye from 100 to 700 mg/L leads to the noticable decline in the MB removal efficiency from 99.9% to 45.3%. In general, once the initial dye concentration is increased, in fact the number of dye molecules in solution increments while the number of the adsorption active sites on the activated carbon is remained unchanged (Bulut and Aydın, 2006). At these conditions, the active sites on the activated carbon surface are fully saturated, therefore, they have no capacity to eliminate all the adsorbate molecules exisiting in the medium, thus, give rise to the mitigation in the dye removal efficiency. Whereas, the adsorption capacity indicated a completely different trend. So that, with increasing the initial dye concentration from 100 to 700 mg/L, the dye absorption capacity was improved from 99.9 to 316.8 mg/g. The substantial mechanism behind such behavior was related to the promoted driving force with the increased initial dye concentration that facilitates the mass transfer. Generally, the more initial adsorbate concentration, the more driving force. As a result, at similar time, more mass of adsorbate molecules is adsorbed on the activated carbon surface in comparision with low initial adsorbate concentrations (Mahmoudi

et al., 2020). The findings attained in this work are consistent with others (Bedin et al., 2016). Based on the outcomes, at initial adsorbate concentrations above 400 mg/L, the content of the adsorption capacity remains somewhat constant, and hence, the concentration of 400 mg/L was regarded as the optimum value.

3.3.5. Contact time

Results obtained from the impact of the contact time (5–240 min) on the dye removal efficiency and the adsorption capacity of the selected activated carbon at optimum conditions (the initial adsorbate concentration of 400 mg/L, the adsorbent dosage of 1.0 g/L, the agitaion speed of 150 rpm and the soltion pH values of 6–7) are indicated in Fig. 7. As clear from the Figure, with the increase in the contact time, the dye removal efficiency and the adsorption capacity improve. The most change in the dye removal efficiency (62.4%) and the adsorption capacity (256.8 mg/g) takes place in the first 5 min of experiments. The high intensity of the adsorption in the first time of experiments is owing to the presence of the large number of empty active sites available on the surface of the activated carbon and the high driving force required for elevating mass transfer (Nizam et al., 2021). By increasing time, lower variations are reported in the dye removal efficiency and the adsorption capacity, so that in 180 min, aformentioned parameters are promoted slightly to 76.9% and 307.45 mg/g, respectively. The cause of reduction in the increasing trend of the mentioned parameters is described by the saturated active sites and the lack of available active sites for adsorbate molecules as well as the mitigation of the driving force because of the decrease in the adsorbate concentration by passing time (Nizam et al., 2021). At contact time above 180 min, the dye removal efficiency and the adsorption capacity remain unchanged. Therefore, the contact time of 180 min was considered as the optimum time. In general, the initial adsorbate concentration of 400 mg/L, the adsorbent dosage of 1 g/L, the agitaion speed of 150 rpm, the soltion pH of 6–7 and the contact time of 3 h at ambient termetature were identified as the optimum conditions for the selected activated carbon.

3.4. Kinetic studies

To evaluate the adsorption rate of dye molecules as adsorbate on the selected activated carbon surface as adsorbent prepared at an activation temperature and time of 900 °C and 60 min, respectively, adsorption kinetics is investigated under optimum adsorption conditions determined in the earlier sections at contact time of 5–240 min (Kumar and Jena, 2016). The data attained from kinetic experiments were modeled with pseudo-first-order, pseudo-second-order and intraparticle diffusion kinetic equations as displayed linearly in Fig. S8. The numerical parameters extracted from these plots are summerized in Table 3. According to aquired results, the pseudo-second-order model with the greatest R^2 (0.9994) denoted the best agreement with the experimental results achived. Further, the value of q_e (equilibrium adsorption capacity) computed from the pseudo-second-order model is similar to that aquired from the adsorption experiments. These findings substantiate that the adsoption process happens chemically involving the exchange of electrons between the adsorbate and the adsorbent. In this mechanism, the amount of the adsorbent and the adsorbate both influences the rate of the adsorption process (Esvandi et al., 2020). As pseudo-first-order and pseudo-second-order models cannot fully characterize the diffusion mechanism, the kinetic data obtained from the intraparticle diffusion model were also analyzed. Totally, if the value of the factor C becomes zero, the adsorption rate is monitored by the intraparticle diffusion. While, in the current study, the value of factor C is larger than zero as revealed in Fig. S8 c. In addition to the chemical adsorption verified by pseudo-second-order model, since the plot of q_t against $t^{0.5}$ is not linear in the entire time interval studied (Figure S8 c), therefore, it can be inferred that the process of physical adsorption is also involved in the adsorption of the MB on the selected AC surface (Hameed and Rahman, 2008). Furthermore, the high rate constant of intraparticle diffusion (K_{ID}) of the selected activated carbon in the adsorption process of the MB molecules confirms formation of good adsorptive bonding between adsorbate and adsorbent particles (Foroutan et al., 2021).

3.5. Adsorption isotherm studies

At equilibrium state, the equations of the adsorption isotherms express how distribution of adsorbed particles between liquid phase (adsorbate solution) and solid phase (adsorbent). The adsorption isotherm studies was performed for the selected activated under optimum adsorption conditions attained in proceeding sections (i.e. contact time of 180 min, adsorbent dosage of 1.0 g/L, solution pH of 6–7, agitation speed of 150 rpm at ambient temperature) in the initial adsorbate concentrations ranging from 100 to 700 mg/L. In the present study, Langmuir, Freundlich and Temkin isotherm models were employed. Graphs and parameters obtained from various isotherms using experimental data are indicated in Figs. S9 and 10 and Table 4. According to the Figures, the linear graphs obtained from different isotherms verify superior fitness of the experimental data with the relevant isotherms. From the results presented in the Table, the most value of correlation coefficient ($R^2 = 0.9999$) belongs to the Langmuir model. According to the research background and high fitness of the experimental data with the Langmuir isotherm, the validity of uniform and monolayer active sites inside the adsorbent surface was proved (Kumar and Jena, 2016). The value of the separation factor (R_L) computed from the Langmuir model is equal to 0.00196, which is in the range of $0 < R_L < 1$, confirming the desirability of concerned isotherm over adsorption process of methylene blue on the selected activated carbon (Armbruster and Austin, 1938). In addition, the value of adsorption intensity calculated from the Freundlich isotherm model is more than one, also exhibiting the desirability of adsorption process (Freundlich, 1906).

3.6. The performance comparison of the selected activated carbon with literature

The use of agricultural residues as precursor has always attracted much attention among specialists and researchers to prepare the activated carbon-based adsorbents owing to having intrinsic attributes like high contents of fixed carbon, volatile matters and lignin, and low amount of ash and moisture. These fabricated activated carbons are employed considerably to eliminate a variety of dyes from aqueous solutions. In this regard, many attempts have been made to enhance the adsorption capacity and specific surface area (S_{BET}) which are the most significant factors in the increase of adsorption process. In summary, the findings attained in this research are compared with others as presented in Table 5. From the Table, the adsorption capacity of the methylene blue as adsorbate and the specific surface area (S_{BET}) of the selected activated carbon in the present research are consistent with the literature.

3.7. The performance investigation of the selected activated carbon as post-treatment of biologically treated wastewaters

In this part of the research, the results of the adsorption experiments related to removal of natural dyes and remained COD along with the adsorption capacity as COD from three types of biologically treated wastewater, namely, effluents from waste stabilization pond (WSP) containing algal dye, licorice processing and baker's yeast wastewaters using the selected activated carbon are presented. In these experiments, the impact of the contact time and adsorbent dosage on the performance of the selected activated carbon in terms of concerned responses from the above-mentioned effluents was studied. Since the natural dyes cover a wide range of colors, the amount of natural dye removal was measured by measuring the adsorption at visible wavelengths (400–800 nm).

Due to the low COD contents of the effluents from the waste stabilization pond and licorice processing wastewater treated biologically, as shown in Table 1, compared to the high MB concentrations, lower adsorbent dosage (0.033, 0.05 and 0.1 g) were used to treat 100 mL of the above-mentioned effluents. While, in the case of the biologically treated baker's yeast processing wastewater due to high effluent COD content (COD of 875.3 mg/L and pH of 7.2–8), higher adsorbent dosages (0.1, 0.2 and 0.3 g) have been used. The contact time is ranged from 15 to 240 min for the three adsorbates.

The results of the natural dye removal efficiency, the residual COD removal efficiency and the adsorption capacity in terms of COD are presented in Fig. 8. According to Fig. 8 a & b, in the first contact time of 15–45 min, complete removal of the algal dye from the effluent of the waste stabilization pond occurred. Obviously, the COD removal efficiency during the adsorption process reached 100% in less than 60 min with the highest dosage of the adsorbent i.e. 0.1 g/100 mL. With decreasing the adsorbent dosage, the COD removal efficiency decreased and the equilibrium time increased. The COD removal efficiency at amounts of 0.033 and 0.05 g and the contact time of 240 min were reported to be 65.9 and 88.6%, respectively. By elevating the adsorbent dosage (ms) from 0.033 to 0.1 g at equilibrium conditions, the amount of the COD adsorption capacity declined from 316.07 to 160.73 mg/g. This reduction is in relation to the increased active sites at the presence of the high dosage of the adsorbent used relative to the number of the dye molecules. As a result, many active sites of the activated carbon remain unused, giving rise to a decline in the adsorption capacity (Nizam et al., 2021).

As clear from Fig. 8 c & d, in general, by rising the value of adsorbent dosage, the dye removal and the COD removal efficiencies from the biologically treated licorice processing wastewater increase. In all three dosages of adsorbent studied, the selected activated carbon is able to eliminate around 100% of the dye. Also, with the increment in the adsorbent dosage from 0.033 to 0.1 g, the COD removal efficiency increases from 51.3 to 100% owing to aforementioned-mechanism (Olusegun and Mohallem, 2020). However, the more increment in the adsorbent dosage from 0.033 to 0.1 g leads to reducing the adsorption capacity in terms of COD from 320.1 to 204.8 mg/g owing to the above described mechanism (Nizam et al., 2021).

The changes trend in the natural dye and COD removal efficiencies from the biologically treated baker's yeast processing wastewater was similar to the biologically treated licorice processing wastewater (Fig. 8g, h and i). So that by increasing the amount of the adsorbent dosage from 0.1 to 0.3 g, the dye removal efficiency and the COD removal efficiency were enhanced from 68.53 to 95.81% and from 45.21 to 91.6%, respectively. On the contrary, the usage of more adsorbent dosage ranged from 0.1 to 0.3 g, the adsorption capacity in terms of COD decreased from 395.72 to 267.26 mg/g owing to the above-mentioned mechanisms.

4. Conclusions

In this study, the different activated carbons (ACs) were prepared physically under CO_2 gas during two separate steps of pyrolysis and activation from walnut shell at various conditions. The impact of the time and temperature at activation stage was investigated on the physicochemical properties (SEM, XRD, FTIR, and BET) and performance of the prepared ACs (as dye removal efficiency and adsorption capacity using methylene blue (MB) as adsorbate). From the obtained findings, the activated carbon prepared at the activation time and temperature of 60 min and 900 °C, respectively, with the highest BET surface area (S_{BET}) (903.91 m^2/g) and adsorption capacity as the MB number (307.45 mg/g) was considered as the selected activated carbon. The adsorption capacity as the iodine number and pH of point of zero charge (pH_{PZC}) of the selected AC were reported to be 1150 mg/g and 6.4, respectively. The functionality of the selected AC was further investigated under varied process conditions as the dye removal efficiency and adsorption capacity of the MB. The highest adsorption capacity under optimum adsorption conditions (initial adsorbate concentration of 400 mg/L, solution pH of 6–7, agitation speed of 150 rpm, adsorbent dosage of 1.0 g/L, and contact time of 180 min at ambient temperature) was achieved to be 307.45 mg/g. From the kinetic and isotherm studies, the selected AC showed the largest conformity with the pseudo-second-order model ($R^2 = 0.999$) and the Langmuir model ($R^2 = 0.9999$), respectively. Accordingly, the adsorption of the MB on the surface of the activated carbon took place uniformly and monolayer. As a final conclusion, the selected AC indicated the best functionality at the adsorbent dosage of 1 g/L with contact time of 240 min for all three colored effluents from waste stabilization pond (WSP), licorice and baker's yeast processing wastewaters biologically treated. The highest value of the adsorption capacity (395.7 mg/g) was related to the adsorption of actual dyes from effluent of biologically treated baker's yeast processing wastewater ascribed to its high levels of COD.

CRediT authorship contribution statement

A. Vakili: Conceptualization, Methodology, Visualization. **A.A. Zinatizadeh:** Supervision, Conceptualization, Visualization, Investigation, Data curation, Writing – review & editing. **Z. Rahimi:** Data curation, Visualization, Investigation, Conceptualization, Methodology, Writing – original draft. **S. Zinadini:** Writing – review & editing. **P. Mohammadi:** Data curation, Writing – review & editing. **S. Azizi:** Data curation, Writing – review & editing. **A. Karami:** Writing – original draft, preparation. **M. Abdulgader:** Writing – review & editing.

Declaration of competing interest

The authors declare that they have no known competing financial interests or personal relationships that could have appeared to influence the work reported in this paper.

Data availability

No data was used for the research described in the article.

Acknowledgment

The authors would like to thank Kermanshah's Water and Wastewater Company, Kermanshah, Iran, for the financial support. The authors also thank Razi University, Kermanshah, Iran, for providing equipped laboratory.

Appendix A. Supplementary data

Supplementary data to this article can be found online at https://doi.org/10.1016/j.jclepro.2022.134899.

References

Abbas, M., Kaddour, S., Trari, M., 2014. Kinetic and equilibrium studies of cobalt adsorption on apricot stone activated carbon. J. Ind. Eng. Chem. 20, 745–751.
Abbas, M., Trari, M., 2020. Removal of methylene blue in aqueous solution by economic adsorbent derived from apricot stone activated carbon. Fibers Polym. 21, 810–820.
Acero, J.L., Javier Benitez, F., Real, F.J., Teva, F., 2012. Coupling of adsorption, coagulation, and ultrafiltration processes for the removal of emerging contaminants in a secondary effluent. Chem. Eng. J. 210, 1–8. https://doi.org/10.1016/j.cej.2012.08.043.
Álvarez-Gutiérrez, N., Gil, M.V., Rubiera, F., Pevida, C., 2015. Cherry-stones-based activated carbons as potential adsorbents for CO2/CH4 separation: effect of the activation parameters. Greenh. Gases Sci. Technol. 5, 812–825. https://doi.org/10.1002/ghg.1534.
Anirudhan, T.S., Ramachandran, M., 2015. Adsorptive removal of basic dyes from aqueous solutions by surfactant modified bentonite clay (organoclay): kinetic and competitive adsorption isotherm. Process Saf. Environ. Protect. 95, 215–225. https://doi.org/10.1016/j.psep.2015.03.003.
Armbruster, M.H., Austin, J.B., 1938. The adsorption of gases on plane surfaces of mica. J. Am. Chem. Soc. 60, 467–475. https://doi.org/10.1021/ja01269a066.

Başar, C.A., 2006. Applicability of the various adsorption models of three dyes adsorption onto activated carbon prepared waste apricot. J. Hazard Mater. 135, 232–241.
Bedin, K.C., Martins, A.C., Cazetta, A.L., Pezoti, O., Almeida, V.C., 2016. KOH-activated carbon prepared from sucrose spherical carbon: adsorption equilibrium, kinetic and thermodynamic studies for Methylene Blue removal. Chem. Eng. J. 286, 476–484.
Benadjemia, M., Millière, L., Reinert, L., Benderdouche, N., Duclaux, L., 2011. Preparation, characterization and Methylene Blue adsorption of phosphoric acid activated carbons from globe artichoke leaves. Fuel Process. Technol. 92, 1203–1212. https://doi.org/10.1016/j.fuproc.2011.01.014.
Beyan, S.M., Prabhu, S.V., Sissay, T.T., Getahun, A.A., 2021. Sugarcane bagasse based activated carbon preparation and its adsorption efficacy on removal of BOD and COD from textile effluents: RSM based modeling, optimization and kinetic aspects. Bioresour. Technol. Reports 14, 100664. https://doi.org/10.1016/j.biteb.2021.100664.
Bhatnagar, A., Anastopoulos, I., 2017. Adsorptive removal of bisphenol A (BPA) from aqueous solution: a review. Chemosphere. https://doi.org/10.1016/j.chemosphere.2016.10.121.
Binh, Q.A., Kajitvichyanukul, P., 2019. Adsorption mechanism of dichlorvos onto coconut fibre biochar: the significant dependence of H-bonding and the pore-filling mechanism. Water Sci. Technol. 79, 866–876. https://doi.org/10.2166/wst.2018.529.
Bulut, Y., Aydın, H., 2006. A kinetics and thermodynamics study of methylene blue adsorption on wheat shells. Desalination 194, 259–267.
Calvete, T., Lima, E.C., Cardoso, N.F., Vaghetti, J.C.P., Dias, S.L.P., Pavan, F.A., 2010. Application of carbon adsorbents prepared from Brazilian-pine fruit shell for the removal of reactive orange 16 from aqueous solution: kinetic, equilibrium, and thermodynamic studies. J. Environ. Manag. 91, 1695–1706. https://doi.org/10.1016/j.jenvman.2010.03.013.
Danish, M., Ahmad, T., 2018. A review on utilization of wood biomass as a sustainable precursor for activated carbon production and application. Renew. Sustain. Energy Rev. https://doi.org/10.1016/j.rser.2018.02.003.
Dawood, S., Sen, T.K., 2012. Removal of anionic dye Congo red from aqueous solution by raw pine and acid-treated pine cone powder as adsorbent: equilibrium, thermodynamic, kinetics, mechanism and process design. Water Res. 46, 1933–1946. https://doi.org/10.1016/j.watres.2012.01.009.
Demiral, H., Demiral, I., Karabacakoğlu, B., Tümsek, F., 2011. Production of activated carbon from olive bagasse by physical activation. Chem. Eng. Res. Des. 89, 206–213. https://doi.org/10.1016/j.cherd.2010.05.005.
Esvandi, Z., Foroutan, R., Peighambardoust, S.J., Akbari, A., Ramavandi, B., 2020. Uptake of anionic and cationic dyes from water using natural clay and clay/starch/MnFe2O4 magnetic nanocomposite. Surface. Interfac. 21, 100754.
Farooq, U., Kozinski, J.A., Khan, M.A., Athar, M., 2010. Biosorption of heavy metal ions using wheat based biosorbents - a review of the recent literature. Bioresour. Technol. https://doi.org/10.1016/j.biortech.2010.02.030.
Fierro, V., Muñiz, G., Basta, A.H., El-Saied, H., Celzard, A., 2010. Rice straw as precursor of activated carbons: activation with ortho-phosphoric acid. J. Hazard Mater. 181, 27–34.
Foo, K.Y., Hameed, B.H., 2012. A rapid regeneration of methylene blue dye-loaded activated carbons with microwave heating. J. Anal. Appl. Pyrolysis 98, 123–128.
Foroutan, R., Mohammadi, R., Farjadfard, S., Esmaeili, H., Ramavandi, B., Sorial, G.A., 2019. Eggshell nano-particle potential for methyl violet and mercury ion removal: surface study and field application. Adv. Powder Technol. 30, 2188–2199. https://doi.org/10.1016/j.apt.2019.06.034.
Foroutan, R., Peighambardoust, S.J., Esvandi, Z., Khatooni, H., Ramavandi, B., 2021. Evaluation of two cationic dyes removal from aqueous environments using CNT/MgO/CuFe2O4 magnetic composite powder: a comparative study. J. Environ. Chem. Eng. 9, 104752.
Freundlich, H.M.F., 1906. Over the adsorption in solution. J. Phys. Chem. 57, 1100–1107.
Ghouma, I., Jeguirim, M., Dorge, S., Limousy, L., Matei Ghimbeu, C., Ouederni, A., 2015. Activated carbon prepared by physical activation of olive stones for the removal of NO2 at ambient temperature. Compt. Rendus Chem. 18, 63–74. https://doi.org/10.1016/j.crci.2014.05.006.
Gokce, Y., Aktas, Z., 2014. Nitric acid modification of activated carbon produced from waste tea and adsorption of methylene blue and phenol. Appl. Surf. Sci. 313, 352–359.
Gupta, V.K., 2009. Application of low-cost adsorbents for dye removal-a review. J. Environ. Manag. 90, 2313–2342.
Gupta, V.K., Kumar, R., Nayak, A., Saleh, T.A., Barakat, M.A., 2013. Adsorptive removal of dyes from aqueous solution onto carbon nanotubes: a review. Adv. Colloid Interface Sci. https://doi.org/10.1016/j.cis.2013.03.003.
Güzel, F., Sayğılı, H., Sayğılı, G.A., Koyuncu, F., Yılmaz, C., 2017. Optimal oxidation with nitric acid of biochar derived from pyrolysis of weeds and its application in removal of hazardous dye methylene blue from aqueous solution. J. Clean. Prod. 144, 260–265.
Hadi, P., Guo, J., Barford, J., McKay, G., 2016. Multilayer dye adsorption in activated carbons-facile approach to exploit vacant sites and interlayer charge interaction. Environ. Sci. Technol. 50, 5041–5049. https://doi.org/10.1021/acs.est.6b00021.
Hameed, B.H., Rahman, A.A., 2008. Removal of phenol from aqueous solutions by adsorption onto activated carbon prepared from biomass material. J. Hazard Mater. 160, 576–581. https://doi.org/10.1016/j.jhazmat.2008.03.028.
Heidari, A., Younesi, H., Rashidi, A., Ghoreyshi, A.A., 2014. Adsorptive removal of CO2 on highly microporous activated carbons prepared from Eucalyptus camaldulensis wood: effect of chemical activation. J. Taiwan Inst. Chem. Eng. 45, 579–588. https://doi.org/10.1016/j.jtice.2013.06.007.
Hindarso, H., Ismadji, S., Wicaksana, F., Mudjijati,Indraswati, N., 2001. Adsorption of benzene and toluene from aqueous solution onto granular activated carbon. J. Chem. Eng. Data 46, 788–791. https://doi.org/10.1021/je000176g.
Ibrahim, T., 2014. Kinetics of the adsorption of anionic and cationic dyes in aqueous solution by low-cost activated carbons prepared from Sea cake and cotton cake. Am. Chem. Sci. J. 4, 38–57. https://doi.org/10.9734/acsj/2014/5403.
Islam, M.A., Ahmed, M.J., Khanday, W.A., Asif, M., Hameed, B.H., 2017. Mesoporous activated coconut shell-derived hydrochar prepared via hydrothermal carbonization-NaOH activation for methylene blue adsorption. J. Environ. Manag. 203, 237–244.
Jia, L., Yu, Y., Li, Z., peng, Qin, S., ning, Guo, J., rong, Zhang, Y., qiang, Wang, J., cheng, Zhang, J., chun, Fan, B., guo, Jin, Y., 2021. Study on the Hg0 removal characteristics and synergistic mechanism of iron-based modified biochar doped with multiple metals. Bioresour. Technol. 332, 125086 https://doi.org/10.1016/j.biortech.2021.125086.
Jiang, W., Xing, X., Li, S., Zhang, X., Wang, W., 2019. Synthesis, characterization and machine learning based performance prediction of straw activated carbon. J. Clean. Prod. 212, 1210–1223. https://doi.org/10.1016/j.jclepro.2018.12.093.
Juang, R.S., Shiau, R.C., 2000. Metal removal from aqueous solutions using chitosan-enhanced membrane filtration. J. Membr. Sci. 165, 159–167. https://doi.org/10.1016/S0376-7388(99)00235-5.
Kannan, N., Sundaram, M.M., 2001. Kinetics and mechanism of removal of methylene blue by adsorption on various carbons-a comparative study. Dyes Pigments 51, 25–40.
Karagöz, S., Tay, T., Ucar, S., Erdem, M., 2008. Activated carbons from waste biomass by sulfuric acid activation and their use on methylene blue adsorption. Bioresour. Technol. 99, 6214–6222.
Karaman, I., Yagmur, E., Banford, A., Aktas, Z., 2014. The effect of process parameters on the carbon dioxide based production of activated carbon from lignite in a rotary reactor. Fuel Process. Technol. 118, 34–41. https://doi.org/10.1016/j.fuproc.2013.07.021.
Kaya, M., Azahin, Ö., Saka, C., 2018. Preparation and TG/DTG, FT-IR, SEM, BET surface area, iodine number and methylene blue number analysis of activated carbon from pistachio shells by chemical activation. Int. J. Chem. React. Eng. 16 https://doi.org/10.1515/ijcre-2017-0060.
Kumar, A., Jena, H.M., 2016. Removal of methylene blue and phenol onto prepared activated carbon from Fox nutshell by chemical activation in batch and fixed-bed column. J. Clean. Prod. 137, 1246–1259. https://doi.org/10.1016/j.jclepro.2016.07.177.
Langmuir, I., 1918. The adsorption of gases on plane surfaces of glass, mica and platinum. J. Am. Chem. Soc. 40, 1361–1403. https://doi.org/10.1021/ja02242a004.
Liu, Q.-S., Zheng, T., Wang, P., Guo, L., 2010. Preparation and characterization of activated carbon from bamboo by microwave-induced phosphoric acid activation. Ind. Crop. Prod. 31, 233–238.
Liu, Y., Guo, Y., Gao, W., Wang, Zhuo, Ma, Y., Wang, Zichen, 2012. Simultaneous preparation of silica and activated carbon from rice husk ash. J. Clean. Prod. 32, 204–209.
Ma, M., Ying, H., Cao, F., Wang, Q., Ai, N., 2020. Adsorption of Congo red on mesoporous activated carbon prepared by CO2 physical activation. Chin. J. Chem. Eng. 28, 1069–1076. https://doi.org/10.1016/j.cjche.2020.01.016.
Mahmoodi, N.M., Hayati, B., Arami, M., Lan, C., 2011. Adsorption of textile dyes on Pine Cone from colored wastewater: kinetic, equilibrium and thermodynamic studies. Desalination 268, 117–125. https://doi.org/10.1016/j.desal.2010.10.007.
Mahmoudi, E., Azizkhani, S., Mohammad, A.W., Ng, L.Y., Benamor, A., Ang, W.L., Ba-Abbad, M., 2020. Simultaneous removal of Congo red and cadmium (II) from aqueous solutions using graphene oxide-silica composite as a multifunctional adsorbent. J. Environ. Sci. 98, 151–160.
Mpatani, F.M., Han, R., Aryee, A.A., Kani, A.N., Li, Z., Qu, L., 2021. Adsorption performance of modified agricultural waste materials for removal of emerging micro-contaminant bisphenol A: a comprehensive review. Sci. Total Environ. https://doi.org/10.1016/j.scitotenv.2021.146629.
Nizam, N.U.M., Hanafiah, M.M., Mahmoudi, E., Halim, A.A., Mohammad, A.W., 2021. The removal of anionic and cationic dyes from an aqueous solution using biomass-based activated carbon. Sci. Rep. 11, 1–17.
Nowicki, P., Pietrzak, R., Wachowska, H., 2010. Sorption properties of active carbons obtained from walnut shells by chemical and physical activation. Catal. Today 150, 107–114. https://doi.org/10.1016/j.cattod.2009.11.009.
Nowrouzi, M., Younesi, H., Bahramifar, N., 2017. High efficient carbon dioxide capture onto as-synthesized activated carbon by chemical activation of Persian Ironwood biomass and the economic pre-feasibility study for scale-up. J. Clean. Prod. 168, 499–509. https://doi.org/10.1016/j.jclepro.2017.09.080.
Oliveira, L.C.A., Pereira, E., Guimaraes, I.R., Vallone, A., Pereira, M., Mesquita, J.P., Sapag, K., 2009. Preparation of activated carbons from coffee husks utilizing FeCl3 and ZnCl2 as activating agents. J. Hazard Mater. 165, 87–94.
Olusegun, S.J., Mohallem, N.D.S., 2020. Comparative adsorption mechanism of doxycycline and Congo red using synthesized kaolinite supported CoFe2O4 nanoparticles. Environ. Pollut. 260, 114019.
Özhan, A., Şahin, Ö., Küçük, M.M., Saka, C., 2014. Preparation and characterization of activated carbon from pine cone by microwave-induced ZnCl2 activation and its effects on the adsorption of methylene blue. Cellulose 21, 2457–2467. https://doi.org/10.1007/s10570-014-0299-y.
Sainz-Diaz, C.I., Griffiths, A.J., 2000. Activated carbon from solid wastes using a pilot-scale batch flaming pyrolyser. Fuel 79, 1863–1871.
Salleh, M.A.M., Mahmoud, D.K., Karim, W.A.W.A., Idris, A., 2011. Cationic and anionic dye adsorption by agricultural solid wastes: a comprehensive review. Desalination 280, 1–13. https://doi.org/10.1016/j.desal.2011.07.019.

Shahkarami, S., Azargohar, R., Dalai, A.K., Soltan, J., 2015. Breakthrough CO2 adsorption in bio-based activated carbons. J. Environ. Sci. (China) 34, 68–76. https://doi.org/10.1016/j.jes.2015.03.008.

Sharafi, K., Mansouri, A.M., Zinatizadeh, A.A., Pirsaheb, M., 2016. Adsorptive removal of methylene blue from aqueous solutions by pumice powder: process modelling and kinetic evaluation. Environ. Eng. & Manag. J. 14 (5), 1067–1078.

Shoaib, M., Al-Swaidan, H.M., 2015. Optimization and characterization of sliced activated carbon prepared from date palm tree fronds by physical activation. Biomass Bioenergy 73, 124–134. https://doi.org/10.1016/j.biombioe.2014.12.016.

Srivastava, V., Maydannik, P., Sharma, Y.C., Sillanpää, M., 2015. Synthesis and application of polypyrrole coated tenorite nanoparticles (PPy@TN) for the removal of the anionic food dye "tartrazine" and divalent metallic ions viz. Pb(II), Cd(II), Zn (II), Co(II), Mn(II) from synthetic wastewater. RSC Adv. 5, 80829–80843. https://doi.org/10.1039/c5ra14108g.

Sumalinog, D.A.G., Capareda, S.C., de Luna, M.D.G., 2018. Evaluation of the effectiveness and mechanisms of acetaminophen and methylene blue dye adsorption on activated biochar derived from municipal solid wastes. J. Environ. Manag. 210, 255–262.

Sun, K., Jiang, J. chun, 2010. Preparation and characterization of activated carbon from rubber-seed shell by physical activation with steam. Biomass Bioenergy 34, 539–544. https://doi.org/10.1016/j.biombioe.2009.12.020.

Theydan, S.K., Ahmed, M.J., 2012. Adsorption of methylene blue onto biomass-based activated carbon by FeCl3 activation: equilibrium, kinetics, and thermodynamic studies. J. Anal. Appl. Pyrolysis 97, 116–122.

Tonucci, M.C., Gurgel, L.V.A., Aquino, S.F. de, 2015. Activated carbons from agricultural byproducts (pine tree and coconut shell), coal, and carbon nanotubes as adsorbents for removal of sulfamethoxazole from spiked aqueous solutions: kinetic and thermodynamic studies. Ind. Crop. Prod. 74, 111–121. https://doi.org/10.1016/j.indcrop.2015.05.003.

Vunain, E., Biswick, T., 2019. Adsorptive removal of methylene blue from aqueous solution on activated carbon prepared from Malawian baobab fruit shell wastes: equilibrium, kinetics and thermodynamic studies. Separ. Sci. Technol. 54, 27–41. https://doi.org/10.1080/01496395.2018.1504794.

Wang, Y., Zhao, L., Peng, H., Wu, J., Liu, Z., Guo, X., 2016. Removal of anionic dyes from aqueous solutions by cellulose-based adsorbents: equilibrium, kinetics, and thermodynamics. J. Chem. Eng. Data 61, 3266–3276. https://doi.org/10.1021/acs.jced.6b00340.

Yagmur, E., Ozmak, M., Aktas, Z., 2008. A novel method for production of activated carbon from waste tea by chemical activation with microwave energy. Fuel 87, 3278–3285. https://doi.org/10.1016/j.fuel.2008.05.005.

Yahya, M.A., Al-Qodah, Z., Ngah, C.W.Z., 2015. Agricultural bio-waste materials as potential sustainable precursors used for activated carbon production: a review. Renew. Sustain. Energy Rev. 46, 218–235. https://doi.org/10.1016/j.rser.2015.02.051.

Yang, J., Qiu, K., 2010. Preparation of activated carbons from walnut shells via vacuum chemical activation and their application for methylene blue removal. Chem. Eng. J. 165, 209–217.

Yazidi, A., Atrous, M., Edi Soetaredjo, F., Sellaoui, L., Ismadji, S., Erto, A., Bonilla-Petriciolet, A., Luiz Dotto, G., Ben Lamine, A., 2020. Adsorption of amoxicillin and tetracycline on activated carbon prepared from durian shell in single and binary systems: experimental study and modeling analysis. Chem. Eng. J. 379 https://doi.org/10.1016/j.cej.2019.122320.

Zangeneh, H., Zinatizadeh, A.A., Zinadini, S., Feyzi, M., Rafiee, E., Bahnemann, D.W., 2019. A novel L-Histidine (C, N) codoped-TiO_2-CdS nanocomposite for efficient visible photo-degradation of recalcitrant compounds from wastewater. J. Hazard Mater. 369, 384–397. https://doi.org/10.1016/j.jhazmat.2019.02.049.

Zhao, H., Yu, Q., Li, M., Sun, S., 2020. Preparation and water vapor adsorption of "green" walnut-shell activated carbon by CO2 physical activation. Adsorpt. Sci. Technol. 38, 60–76. https://doi.org/10.1177/0263617419900849.